Available online at www.sciencedirect.com

ScienceDirect

Mendeleev Commun., 2022, **32**, 28–32

Mendeleev Communications

η^2-Phosphasilene transition metal complexes – a novel building block for hetero-multimetallic complexes

Boris Minkovich, Alexander Kaushansky, Natalia Fridman, Dmitry Bravo-Zhivotovskii* and Yitzhak Apeloig*

Schulich Faculty of Chemistry, Technion – Israel Institute of Technology, 32000 Haifa, Israel.
E-mail: apeloig@technion.ac.il; chrbrzh@technion.ac.il

DOI: 10.1016/j.mencom.2022.01.008

Compound η^2-$((R_3Si)_2Si{=}PH)$–Pt(dmpe) was synthesized by trapping the transient phosphasilene, $(R_3Si)_2Si{=}PH$. Novel hetero-bi- and tri-metallic complexes derived from η^2-$((R_3Si)_2Si{=}PH)$–Pt(dmpe) containing Pt with Li, Zn, Hg and Ag metals were synthesized and characterized by multinuclear NMR spectroscopy and X-ray crystallography. The synthesis of η^2-$((R_3Si)_2Si{=}PH)$–Pt(dmpe), and its bonding character are discussed; a 1,2-silyl shift from silicon to phosphorus (a 'Brook-type' rearrangement) within the coordination sphere of a Pt complex is also reported.

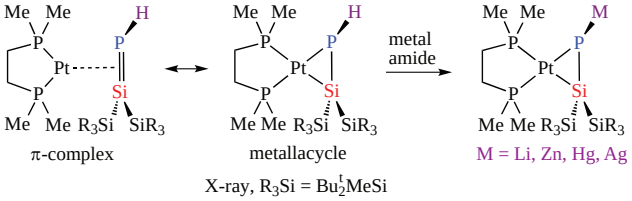

Keywords: silicon, phosphorus, phosphasilene, heavy main-group multiple bonds, hetero-bimetallic complex, π-complex, transition metal complex, NMR, X-ray structures.

Transition metal (TM) alkene and alkyne complexes are well-studied valuable compounds.[1–5] More recently their heavy analogs, *i.e.*, η^2-complexes of TM with E=E′ (E, E′ = C, Si, Ge, Sn, Pb), were also reported.[4,6] TM complexes of unsaturated hetero atom compounds (such as C=N and C=P) are valuable and versatile ligands used in catalysis.[7,8] Multi-metallic complexes attracted in recent years great attention, aiming to gain more efficient/selective catalysts.[9,10] Inspiration comes from Nature, attempting to mimic the cooperative properties of metalloenzymes containing two or more metals.[11] Thus, a search for superior polydentate ligands continues to attract the interest of many researchers.

Phosphasilene ($R_2Si{=}PH$), a heavier analog of a C=P ligand, is an interesting ligand for synthesizing multimetallic TM complexes (Figure 1). Recently, TM–phosphasilene complexes of types **A**,[12–14] **B**,[15] and **C**[16] were reported, exhibiting the versatile coordination abilities of phosphasilenes. A close relative of phosphasilene, *viz*. phosphinosilylene, was used as a ligand in hetero-bimetallic complexes **D**.[17] The ability of $R_2Si{=}PH$ to be a reactive double bond which can form a (η^2) TM π-complex as in **C** was demonstrated by Driess.[16] However, $R_2Si{=}PH$ has two additional functions, the P–H bond (H can be substituted by M_2) and the P lone pair which can coordinate to M_3. Thus, $R_2Si{=}PH$ is a potential precursor for synthesizing novel hetero-bi- or tri-metallic complexes of types **E** and **F**, respectively. Such complexes are not yet known, to the best of our knowledge. Herein, we report the synthesis and characterization of the first isolated compounds of types **E** and **F**.

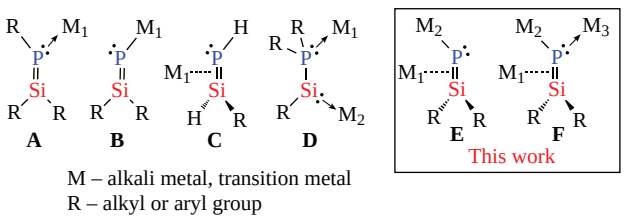

Figure 1 Multimetallic transition metal (TM) complexes **A**–**F**.

To obtain the desired $R_2Si{=}PH$ ligand **3**, precursor **1** was first synthesized from Na_3P and $(Bu^t{}_2MeSi)_2SiF_2$.[18] Addition of LDA to **1** yields quantitatively the lithium salt **2** (Scheme 1, stage i). Disappointingly, phosphide **2** is stable in THF even upon heating to 70 °C and elimination to give **3** is not observed. Changing the THF solvent to hexane yields a complex mixture of products. 3. As the formation of **3** from **2** by elimination of LiF was not successful, we attempted to generate **3** *in situ* and to trap it with a TM complex. Reaction of lithium phosphide **2** with $(dmpe)Pt(Et_3P)_2$ [dmpe is 1,2-bis(dimethylphosphino)ethane] in a 1:1 THF/hexane solvent affords the desired η^2-$(R_2Si{=}PH)$–Pt(dmpe) functional complex **4** (see Scheme 1, stage ii), accompanied by eliminated LiF. The overall crude yield of **4** from **1** is *ca*. 60% (20% after purification by crystallization). Compound **4** was characterized by NMR spectroscopy and X-ray crystallography (for details, see Online Supplementary Materials).

Inspired by earlier work of West and Pham, in which η^2-disilene platinum complexes were synthesized by oxidative addition of a L_2Pt^0 complex to a Si–H bond of 1,2-dihydrodisilanes followed by elimination of H_2,[19,20] we carried out reaction of compound **5**[18] with $(dmpe)Pt(Et_3P)_2$. After a week in hexane at 60 °C, product **4** is cleanly formed *via* H_2 elimination from the proposed intermediate **6** (not observed) (see Scheme 1, stage iii). Compound **4** crystallizes from the reaction mixture upon concentration of the solution in an isolated yield of 85%. So, this procedure for the synthesis of **4** is far superior to that in stages i–ii.

The bonding of an alkene to a transition metal is understood in terms of the Dewar–Chatt–Duncanson model.[21,22] According to this model, two major bonding interactions are involved:

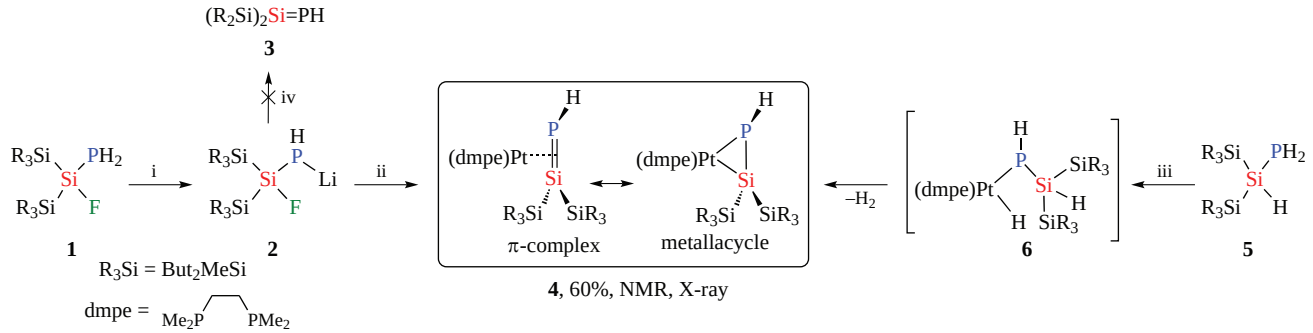

Scheme 1 *Reagents and conditions*: i, LDA, THF, room temperature, 5 min; ii, (dmpe)Pt(Et_3P)$_2$, 1:1 hexane/THF, 65 °C, 3 days; iii, (dmpe)Pt(Et_3P)$_2$, hexane, 60 °C, 1 week; iv, THF, 70 °C, 2 h, no reaction, solvent change to hexane leads to complex mixture.

(*a*) alkene-to-metal σ-donation (*via* the π-bond electrons) and (*b*) metal-to alkene π-back donation into the alkene's π* empty orbital.[23] The structure of an alkene–TM complex is significantly influenced by the relative importance of σ-donation *versus* π-back donation.[23] Accordingly, these complexes are classified into two groups: a π-complex having major contribution of σ-donation, or a metallacycle in which π-back donation is dominant (see Scheme 1). In π-type complexes the geometry around the alkene ligand is not very different from that of the free alkene, while in metallacycles the geometry is significantly distorted from that of the alkene with an elongated C–C bond and a large bent angle at the alkene carbon atoms.[23]

In addition to **4**, η^2-(Si=PH)–Pt(dmpe) complexes **7**–**9** with different phosphine ligands were synthesized to gain better understanding of the bonding in these complexes. Compounds **7**–**9** were prepared similarly to **4** and were analyzed by NMR spectroscopy (see Online Supplementary Materials). Unfortunately, no crystal structures are available for complexes **7**–**9**.

In complexes **4**, **7**–**9** the characteristic ^{31}P and ^{29}Si NMR signals of the Si–P fragment are strongly upfield shifted (Figure 2), compared to free $(R_3Si)_2Si=PR'$ with similar R_3Si substituents on Si and R′ = Mes* (^{31}P: +389 ppm, ^{29}Si: +201 ppm).[24] The observed upfield shift in the Pt-complexes, as a function of the substituents on Pt, follows the order (Table 1): Ph_3P (**9**) → dppe [dppe is 1,2-bis(diphenylphosphino)ethane] (**8**) → Et_3P (**7**) → dmpe (**4**) (most upfield). This trend is consistent with the Dewar–Chatt–Duncanson model.[21–23] Thus, the trend follows the σ-basicity of the phosphine ligands: (dmpe > Et_3P > dppe > Ph_3P)[25] *i.e.*, stronger σ-donation from the P-ligand (the stongest σ-donor is dmpe) to Pt leads to stronger π-back donation to the π* (Si=P) orbital. Thus, according to the NMR data, complexes **4**, **7**–**9** can be described as metallacycles with only a small π-complex character. This conclusion is supported by the X-ray structure of **4**, discussed below.

Complex **4** crystallizes from pentane as light green rhombic crystals and its molecular structure was determined by X-ray crystallography (Figure 3).† The X-ray structure shows a relatively long Si–P bond (2.23 Å), which is 5.7% longer than the longest reported Si=P bond of 2.11 Å, in

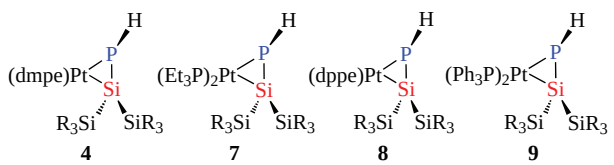

	4	**7**	**8**	**9**
^{29}Si/ppm	–54.2	–50.4		–44
^{31}P/ppm	–205	–179.3	–179.7	–143.8

Figure 2 ^{29}Si NMR and ^{31}P NMR chemical shifts for **4**, **7**–**9**.

($Bu^t_2MeSi)_2Si=P–Mes*$.[24] The bent-back angle [defined as the angle between the Si(2)–Si(1)–Si(3) plane and the Si(1)–P(3) bond] describing the distortion of the double bond substituents from its ideal planar geometry in the free $R_2Si=PH$ in **4**, is 23.9°. Both the long Si–P bond and the large bent angle denote strong π-back donation from Pt into the π*(Si=P) empty orbital and indicate a metallacycle structure.

To evaluate further the effect of the phosphine ligands on the Si–P bond length [*r*(Si–P)] and the Si–P bond order (WBI – Wiberg Bond Index), quantum mechanical Density Functional Theory (DFT) calculations were performed (at the B3LYP/6-311+G(d,p)/LANL2DZ on Pt) for model compounds: $(Me_3Si)_2Si=PH$, **A**; $L_xPt[(Me_3Si)_2Si=PH]$, L = Ph_3P, **B**; dppe, **C**; Me_3P, **D**; dmpe, **E** (Figure 4).‡ The calculated WBI of 1.92 for the non-complexed **A**, indicates a nearly full P=Si double bond character. Upon TM complexation the WBI of the Si–P bond drops substantially to *ca*. 1.2 for complexes **B**–**E**, indicating that complexes **B**–**E** have primarily a metalacyclic character. The same conclusion is reached by examining the calculated Si–P bond lengths, which are elongated from 2.106 Å in non-complexed **A** to 2.229–2.237 Å in complexes **B**–**E**, within the typical range of Si–P single bonds.[20] There are no significant changes in the Si–Pt and P–Pt bond lengths along the **B**–**E** series.[20] The calculated WBI values and bond lengths are consistent with the experimental NMR trends discussed above

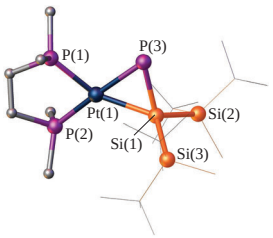

Figure 3 X-ray crystallography molecular structure of **4** (Olex drawing). Hydrogen atoms are omitted for clarity.

† Crystallographic and structural details are given in Online Supplementary Materials. Full details of the X-ray crystallography structures are given in CCDC 2110513 (**4**), 2116257 (**10**), 2110514 (**12**), 2110516 (**13a**), 2110550 (**14**), 2110515 (**15**). The data can be obtained free of charge from The Cambridge Crystallographic Data Centre *via* http://www.ccdc.cam.ac.uk.

‡ All calculations were carried out using Gaussian 09 Rev. D1 software using Density Functional Theory (DFT). The calculations were carried out at the B3LYP/6-311+G(d, p) (for H, C, Si, P, O) level, Pt was described with LANL2DZ. The optimized minima and transition state were verified by harmonic vibrational analysis to have no imaginary frequency and one proper imaginary frequency, respectively. The transition-state structure was confirmed to connect corresponding reactant and product by intrinsic reaction coordinate (IRC) calculations. Further computational details and a full reference list for the methods used are provided in Online Supplementary Materials.

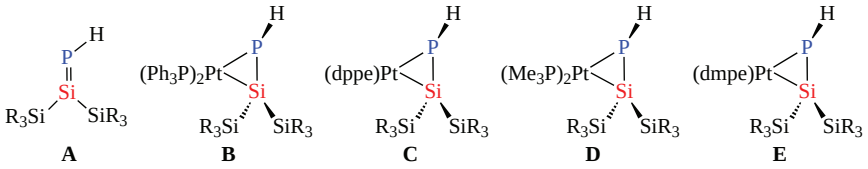

	A	**B**	**C**	**D**	**E**
WBI(Si–P)	1.92	1.22	1.21	1.21	1.20
r(Si–P)/Å	2.106	2.229	2.235	2.232	2.237
r(Si–Pt)/Å		2.401	2.398	2.399	2.402
r(P–Pt)/Å		2.508	2.491	2.508	2.491

Figure 4 Calculated bond lenghts and Winerg Bond Index (WBI) values for complexes **A**–**E**.

for complexes **4**, **7**–**9**, and the proposed effect of the phosphine ligands' σ-basicity on the Pt–(Si=P) bonding nature. The results are also consistent with previously reported data on complexes of this type.[6,12,16]

Metalation of the P–H bond in a (R_2Si=PH)–Pt(dmpe)-complex converts the complex to a reactive building block (**E** in Figure 1). To our best knowledge, such complexes, containing a η^2-Pt–(Si=P–Li) unit, were not previously reported. Reaction of **4** with LDA in hexane overnight results in color change from pale yellow to bright orange (Scheme 2). Multi-nuclear NMR analysis reveals quantitative conversion of **4** to a new complex **10**, which was confirmed by X-ray crytallography. The NMR signals of **10** are broad and poorly resolved, a common behaviour of R–Li species in poor solvating media.[26]

Compound **10** crystallizes as red crystals upon concentration of the reaction mixture. The X-ray analysis reveals [Figure 5(*a*)]† a unit cell containing four (R_2Si=PLi)–Pt(dmpe) complexes co-crystallized with Li_2O (which may originate from residual moisture) forming Li_4 square cycle with O atom at the center. The Si–P bond lengths (2.179–2.206 Å) are slightly shorter compared to **4**, with only small additional influence on the bond angles and bond lengths within the Pt–Si and Pt–P fragments. The P–Li bond lengths in **10** vary from 2.344 to 3.303 Å.

The molecular structure of **10** is confirmed by chemical transformations. Its hydrolysis yields the expected precursor complex **4** (see Scheme 2). Compound **10** also rapidly reacts with Me_3SiCl at room temperature to produce the P-silylated complex **11**. Interestingly, addition of THF to **10** affords unexpectedly a new complex **12**, an isomer of **4**, obtained *via* silyl group 1,2-shift from ring Si(2) to phosphorus P(3). This is the first example of a 1,2-silyl shift from silicon to phosphorus ('Brook[27]–West[28]-type' rearrangement) within the coordination sphere of a transition metal. The X-ray structure of complex **12** [Figure 5(*b*)] shows that the Si(2)–P(3) bond (2.193 Å) is by 0.04 Å shorter than in **4** (2.23 Å), but it is 3.79% longer than the longest Si=P bond reported (2.11 Å[24]). The Pt–P and Pt–Si distances are very similar in **4** and **12**. Thus, compound **12**,

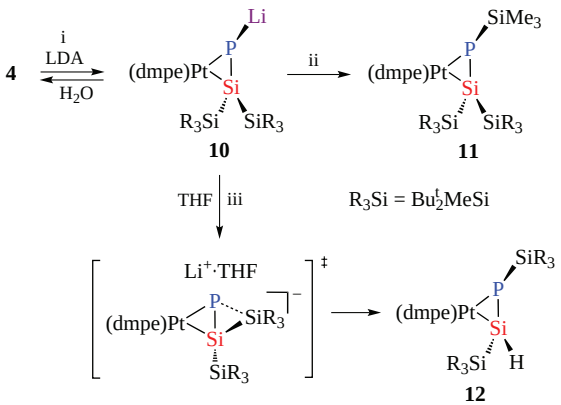

Scheme 2 *Reagents and conditions*: i, LDA, hexane, room temperature, overnight; ii, TMS_3SiCl, hexane, room temperature, 5 min; iii, THF, room temperature, 5 min.

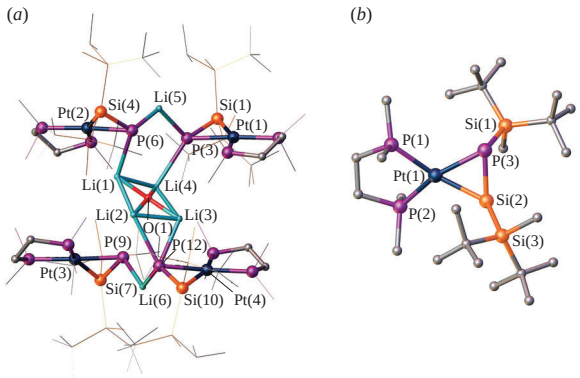

Figure 5 X-ray crystallography molecular structures of (*a*) compound **10** and (*b*) compound **12** (Olex drawing). Hydrogen atoms are omitted for clarity.

similarly to **4**, is best described as a metallacycle. The two bulky silyl substituents in **12** are nearly *anti* to each other with a Si(1)–P(3)–Si(2)–Si(3) dihedral angle of 141.1°.

DFT calculations (at B3LYP/6-311G+(d,p)/LANL2DZ [Pt], PCM (THF), level of theory) were carried out to examine the transformation of **4** to **12** (Figure 6). The calculations were performed on a model system in which the Bu^t_2MeSi groups are modeled by H_3Si groups, and the base is Me_2N^-. The conversion of precursor **i** to the rearranged product **v** is slightly exergonic, by 2.7 kcal mol^{-1}. Rearrangement starts from anion **ii**. The cyclic transition state TS**iii** for the isomerization, in which the migrating silyl group bridges the Si–P bond, lies by ($\Delta G^{\ddagger}$) 25.5 kcal mol^{-1}

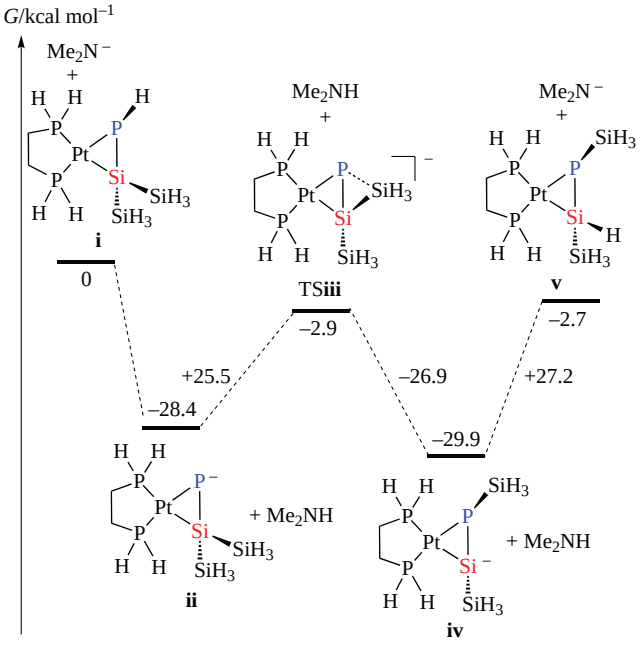

Figure 6 Calculated free energies for the rearrangment of **i** to **v** *via* transition state **iii**.

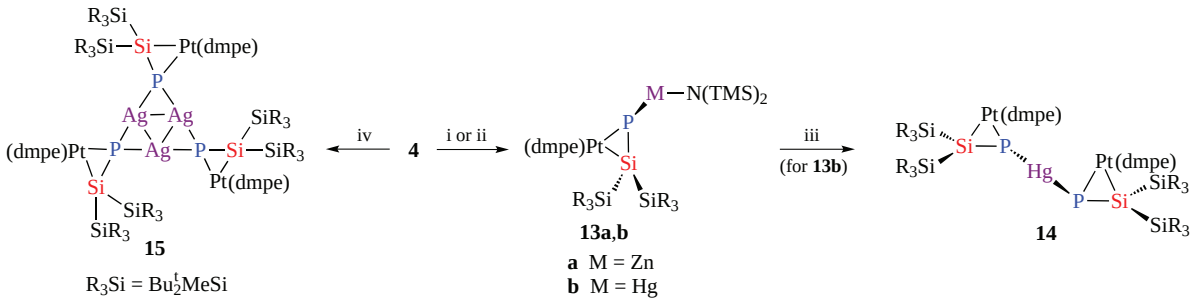

Scheme 3 *Reagents and conditions*: i, $(TMS_2N)_2Zn$, hexane, 75 °C, 6 days; ii, $(TMS_2N)_2Hg$, hexane, room temperature, overnight; iii, Li metal, hexane, room temperature, 72 h; iv, $(TMS_2N)Ag$, hexane, room temperature, overnight.

above **ii**. The rearranged anion **iv** is by only 1.5 kcal mol^{-1} more stable than **ii**. The protonated rearranged complex **v** is by 27.2 kcal mol^{-1} higher in energy than its Si-anion **iv**. Experimentally we cannot isolate the rearranged Si-Li species due to its immediate protonation by free amine present in the reaction mixture (from the reaction of **4** with LDA), shifting the equilibrium to the rearranged protonated product.

Compound **4** can be metalated at P also with transition metal amides such as $(TMS_2N)_2Zn$, $(TMS_2N)_2Hg$ and $(TMS_2N)Ag$ (Scheme 3). Reaction of **4** with $(TMS_2N)_2Zn$ yielding the P–Zn complex **13a**, is relatively slow requiring prolonged heating at 75 °C for 6 days.

Compound **13a** crystallizes from hexane solution as yellow rhombuses. The X-ray molecular structure (Figure 7)† is monomeric, and the structure, in particular the Pt–(P–Si) ring, is only little affected by the Zn substituent; *r*(Si–P) = 2.225 Å, *r*(P–Zn) = 2.220 Å, and the other bonds are in the range of typical single bonds of similar type. The phosphorus atom [P(3)] is pyramidal (sum of angles is 236.98°), so the P lone pair is not involved in binding the Zn atom. The ^{31}P NMR spectrum shows a signal at –199.2 ppm (corresponding to a P atom substituted with Si), as a doublet of doublets (splitting caused by the *cis*- and *trans*-located phosphine groups of the dmpe ligand), accompanied by ^{195}Pt satellites with $^1J_{Pt,\,P}$ = 115 Hz (see Online Supplementary Materials).

Reaction of compound **4** with $(TMS_2N)_2Hg$ (hexane, room temperature) smoothly produces complex **13b** (see Scheme 3). The ^{31}P NMR spectrum shows a peak at –161.74 ppm (corresponding to a P atom substituted with Si), as a doublet of doublets (splitting caused by the *cis*- and *trans*-located phosphine groups of the dmpe ligand), accompanied by ^{195}Pt satellites with J_{PtP} = 112 Hz and ^{199}Hg satellites with $J_{Hg,P}$ = 1439.19 Hz (see Online Supplementary Materials). Reaction of **13b** with Li metal in hexane leads to precipitation of yellow crystals (see Scheme 3). The ^{31}P NMR of the reaction mixture shows that **13b** was fully consumed, but the product was not soluble and thus a NMR spetrum could not be recorded. The structure of the product **14** was understood only after X-ray analysis (see Figure 7), which revealed symmetrical, almost linear P–Hg–P core, with a P–Hg–P angle of 171.5°, and *r*[P(1),P(2)–Hg(1)] of 2.404 Å. The P(1)–Si(1) and P(2)–Si(4) bonds of 2.24 Å and the other bonds are in the range of similar complexes. The phosphorus atoms are pyramidal (∑∠P = 210.32°) and their lone pairs are not involved in bonding, pointing outwards from the (P–Si)–Pt rings.

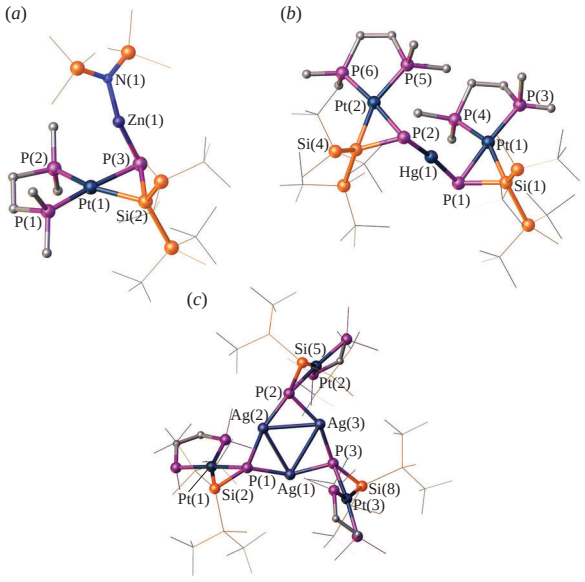

Figure 7 X-ray crystallography molecular structures of compounds (*a*) **13a**, (*b*) **14** and (*c*) **15** (Olex drawing). Hydrogen atoms are omitted for clarity.

Overnight reaction of **4** with $(TMS_2N)Ag$ leads to quantitative conversion to a new Ag-containing complex **15** (see Scheme 3). The ^{31}P NMR spectrum of the reaction mixture shows the presence of at least two different but very similar complexes in a 2 : 1 ratio. Their ^{31}P NMR peaks at –185.6 and –194.6 ppm are split by the *cis* and *trans* P-atoms of the dmpe ligand, and are accompanied by ^{107}Ag satellites $^1J_{AgP}$ = 846 and 910 Hz. The peaks are broad, thus, the ^{135}Pt satellites cannot be determined. The broad split peaks indicate an aggregated cluster structure. Complex **15** crystallizes from hexane as yellow-green crystals which comprise unique Pt–P–Ag aggregated cluster of three molecules (see Figure 7), which provides an explanation also for the NMR spectrum. Thus, the three units are not identical, and apparently, the lack of symmetry present in the Ag_3-cluster persists also in the solution. In the solid state, the three P and three Ag atoms are nearly in the same plane. The silver substitution at P does not affect the Pt-complex backbone distances which remains almost identical to those in **4**. The P–Ag bond lengths are 2.38–2.44 Å, which are in typical P–Ag distance range.[29] The Ag–Ag distances are 3.077(4)–3.304(2) Å, significantly longer than the sum of the metallic radii of two Ag atoms (2.884 Å); hence, **15** has no formal Ag–Ag covalent bonds.[30] Interestingly, the P–Ag–P angles are 152.9–164.4°, significantly deviating from the common linear geometry at Ag. This can be explained by the Ag_3P_3 ring strain, dictated by the acute Ag–P–Ag angles (79.2–86.4°).

Complexes **13a**,**b** and **14** are examples of unique hetero-bimetallic, while **10** and **15** are hetero-trimetallic compounds (in the solid state). The bridging ligand, a reactive transient phosphasilene trapped *in situ* by the transition metal (Pt), provides a rigid geometry around the transition metal center and bears two additional coordination sites: the P–H bond, which was utilized in this study, and the P lone pair which still can be used to coordinate a third metal. Complex **4** proved to be a useful precursor for preparing a variety of novel hetero-bi- and tri-metallic complexes. The reactions and potential use of these novel multi-metallic catalysts are under current study.

This study was supported by the Technion's Research Fund.

Online Supplementary Materials

Supplementary data associated with this article can be found in the online version at doi: 10.1016/j.mencom.2022.01.008.

References

1 G. Wilke and G. Herrmann, *Angew. Chem.*, 1962, **74**, 693.
2 C. D. Cook and G. S. Jauhal, *Inorg. Nucl. Chem. Lett.*, 1967, **3**, 31.
3 R. van der Linde and R. O. de Jongh, *J. Chem. Soc. D*, 1971, 563.
4 F. Nunzi, A. Sgamellotti, N. Re and C. Floriani, *J. Chem. Soc., Dalton Trans.*, 1999, 3487.
5 B. F. Straub, *Angew. Chem., Int. Ed.*, 2010, **49**, 7622.
6 S. Ishida and T. Iwamoto, *Coord. Chem. Rev.*, 2016, **314**, 34.
7 K. C. Gupta and A. K. Sutar, *Coord. Chem. Rev.*, 2008, **252**, 1420.
8 J. I. Bates, J. Dugal-Tessier and D. P. Gates, *Dalton Trans.*, 2010, **39**, 3151.
9 M. Delferro and T. J. Marks, *Chem. Rev.*, 2011, **111**, 2450.
10 P. Buchwalter, J. Rosé and P. Braunstein, *Chem. Rev.*, 2015, **115**, 28.
11 B. L. Feringa, O.-J. Gelling, M. T. Rispens and M. Lubben, in *Transition Metals in Supramolecular Chemistry*, eds. L. Fabbrizzi and A. Poggi, Springer, Netherlands, 1994, pp. 171–190.
12 V. Nesterov, N. C. Breit and S. Inoue, *Chem. – Eur. J.*, 2017, **23**, 12014.
13 B. Li, T. Matsuo, T. Fukunaga, D. Hashizume, H. Fueno, K. Tanaka and K. Tamao, *Organometallics*, 2011, **30**, 3453.
14 K. Hansen, T. Szilvási, B. Blom and M. Driess, *Organometallics*, 2015, **34**, 5703.
15 M. Driess, S. Block, M. Brym and M. T. Gamer, *Angew. Chem., Int. Ed.*, 2006, **45**, 2293.
16 T. J. Hadlington, T. Szilvási and M. Driess, *J. Am. Chem. Soc.*, 2019, **141**, 3304.
17 N. C. Breit, C. Eisenhut and S. Inoue, *Chem. Commun.*, 2016, **52**, 5523.
18 N. Wiberg, W. Niedermayer, H. Nöth, J. Knizek, W. Ponikwar, K. Polborn, D. Fenske and G. Baum, *Z. Anorg. Allg. Chem.*, 2001, **627**, 594.
19 E. K. Pham and R. West, *J. Am. Chem. Soc.*, 1989, **111**, 7667.
20 E. K. Pham and R. West, *Organometallics*, 1990, **9**, 1517.
21 M. J. S. Dewar, *Bull. Soc. Chim. Fr.*, 1951, C71.
22 J. Chatt and L. A. Duncanson, *J. Chem. Soc.*, 1953, 2939.
23 *Modern Coordination Chemistry*, eds. G. J. Leigh and N. Winterton, Royal Society of Chemistry, Cambridge, 2002.
24 V. Ya. Lee, M. Kawai, A. Sekiguchi, H. Ranaivonjatovo and J. Escudié, *Organometallics*, 2009, **28**, 4262.
25 T. Iwamoto, Y. Sekiguchi, N. Yoshida, C. Kabuto and M. Kira, *J. Chem. Soc., Dalton Trans.*, 2006, **60**, 177.
26 L. D. McKeever and R. Waack, *J. Chem. Soc. D*, 1969, 750.
27 A. G. Brook, *J. Am. Chem. Soc.*, 1958, **80**, 1886.
28 A. Wright and R. West, *J. Am. Chem. Soc.*, 1974, **96**, 3214.
29 S. Nawaz, A. A. Isab, K. Merz, V. Vasylyeva, N. Metzler-Nolte, M. Saleem and S. Ahmad, *Polyhedron*, 2011, **30**, 1502.
30 W. Suning, J. P. Fackler, Jr., and T. F. Carlson, *Organometallics*, 1990, **9**, 1973.

Received: 7th October 2021; Com. 21/6719